Robotica (2017) volume 35, pp. 2297–2318. © Cambridge University Press 2017
doi:10.1017/S0263574716000886

Modeling and control of an underactuated tractor–trailer wheeled mobile robot

Asghar Khanpoor†, Ali Keymasi Khalaji‡* and S. Ali A. Moosavian†

† *Department of Mechanical Engineering, K. N. Toosi University of Technology, Tehran, Iran.*
E-mails: asghar.khanpoor@yahoo.com, moosavian@kntu.ac.ir
‡ *Department of Mechanical Engineering, Engineering Faculty, Kharazmi University, Tehran, Iran*

(Accepted December 20, 2016. First published online: January 31, 2017)

SUMMARY
Trajectory tracking is one of the main control problems in the context of Wheeled Mobile Robots (WMRs). Control of underactuated systems has been focused by many researchers during past few years. In this paper, tracking control of a Tractor–Trailer Wheeled Mobile Robot (TTWMR) has been discussed. TTWMR includes a differential drive WMR towing a passive spherical wheeled trailer. Spherical wheels in contrast with standard wheels make the robot highly underactuated with severe non-linearities. Underactuation is due to the use of spherical wheeled trailer to increase robots' maneuverability and degrees of freedom. In fact, standard wheels are subjected to non-holonomic constraints due to pure rolling and non-slip conditions, which reduce robot maneuverability. In this paper, after introducing the robot, kinematics and kinetics models are obtained. Then, based on a physical intuition, a novel control algorithm is developed for the robot, i.e. Lyapunov-PID control algorithm. Subsequently, singularity avoidance of the proposed algorithm is discussed and the stability of the algorithm is analyzed. Finally, simulation and experimental results are presented which reveal the effectiveness of the proposed algorithm.

KEYWORDS: Tractor–trailer wheeled mobile robot, Trajectory tracking, Non-holonomic system, Underactuation, Lyapunov theorem.

Nomenclature

$A(q)$	Constraint Matrix
a_1	Length of PC_1
a_{jk}	Constraint Multipliers
c_i	Center of Gravity for Tractor and Trailer
c_t	Spiral Damping Ratio
$E(q)$	Input Conversion Matrix
e	Generalized Coordinate Error vector
f	Run Force of Tractor
$G(q)$	Gravity Matrix
J_i	Inertia of tractor and Trailer
k_t	Spiral Spring Ratio
k_p	Proportional Gain of PID-action
k_i	Integral Gain of PID-action
k_d	Derivative Gain of PID-action
l	Length of PC_2
m_i	Mass of Tractor and Trailer
$M(q)$	Inertia Matrix

* Corresponding author. E-mail: keymasi@khu.ac.ir

P	Middle Point of Tractor Axle
q	Generalized Coordinate Vector
r	Radius of Actuated Tractor Wheels
$\dot{s}$	Velocity of Point P
$S(q)$	Jacobian Matrix
$T(q, \dot{q})$	Kinetic Energy of System
u	Kinematic Input Vector
$U(q)$	Potential Energy of System
$V(q, \dot{q})$	Carioles Matrix
$V(e)$	Lyapunov Function
x, y	Location of Point P
z	State Variables Vector
$\mathcal{L}(q, \dot{q})$	Lagrangian
λ	Lagrange Multipliers
$\beta_i \gamma_i$	Corrective Terms
τ	Orientation Torque of Tractor
θ_i	Orientation of Tractor and Trailer
ω_l	Tractor Left Wheel Rotational Velocity
ω_r	Tractor Right Wheel Rotational Velocity
ζ	Workspace Variables

1. Introduction

Wheeled Mobile Robots (WMRs) applications are growing in manufacturing and robotic services, particularly when flexible motion capabilities are required on reasonably smooth grounds and surfaces. The wheel is the most popular locomotion mechanism in mobile robotics and in man-made vehicles due to its simplicity, efficiency and flexibility. Numerous mobility configurations (wheel numbers, types and locations, sensing and actuation, single or multi-body vehicle structure) can be found for WMRs locomotion. In addition, mechanical stability is not usually a research problem in wheeled robots design, because wheeled robots are almost always designed so that all wheels are in ground contact all the time. Thus, three wheels are sufficient to guarantee stable motion of the robot.[1] So, dynamics and control of these systems were studied by many researchers during past decades.[2–4] Dynamics and structural specifications of a variety of WMRs were discussed in ref. [5]. WMRs due to the pure rolling and non-slip conditions are subjected to non-holonomic constraints. Non-holonomic constraints are limitations in velocity and acceleration levels. In other words, these constraints reduce the system degrees of freedom in velocity and acceleration levels without change in degrees of freedom in displacement level. In addition to increasing complexities in modeling and control, non-holonomic constraints raise the interesting features of these systems. N. I. Kolmanovsky[6] presented an overview of control methods has been presented. Control of non-holonomic systems has been focused on various motion tasks including path following,[7,8] point stabilization[9,10] and trajectory tracking.[11,12] E. Yang *et al.*[13] after obtaining dynamics model of a car-like robot which has two non-holonomic constraints, achieved a non-linear tracking controller using the dynamic feedback linearization technique. C. Y. Chen *et al.*[14] proposed an adaptive sliding-mode dynamic controller for WMRs is designed to implement trajectory tracking mission. J. Huang *et al.*[15] investigated an adaptive output feedback tracking controller for WMRs to guarantee that tracking errors are confined to an arbitrarily small ball. D. Chwa[16] presented a fuzzy adaptive tracking control method for WMRs, where unknown slippage occurs and violates the non-holonomic constraint in the form of state-dependent kinematic and dynamic disturbances. The control problems are mostly studied on dynamics modeling and control of unicycle or carlike mobile robots, while there are few works on WMRs attached by passive trailers. The delivery and transportation capacity can be increased via trailers. Also, the cost of the robot with trailers is much lower than the cost of multiple robots. The purposes of control studies for tractor–trailer wheeled robots are different from motion aid in human-driven transportation and delivery systems, to fully autonomous navigation in multi-body mobile robotics. However, the major drawback of the trailer systems is that the control problem is difficult.

A tractor–trailer system with spherical wheels is an underactuated non-holonomic system which can be seen in snake-like robots with high degrees of freedom. These systems have high agility

https://doi.org/10.1017/S0263574716000886 Published online by Cambridge University Press

to move in clumsy environments such as through pipelines for inspection or cleaning, underwater applications and so on. Actuating all system segments results in higher weights and volumes for the system. By reducing the number of actuators and using an appropriate control algorithm, without reducing the number of system segments, one could have a mechanism with enough agility and at the same time have a system with lower consumption of energy.

A mechanical system may become underactuated due to several reasons. The most obvious way is the intentional design as in the passive walker of the McGeer.[17] Underactuation also arises in robotic manipulators, for example, when a manipulator arm is attached to a mobile platform, space platform, or an underwater vehicle.[18] The third way that underactuation arises is due to the mathematical model used for control design, for example, when joint flexibility is included in the model.[19] M. W. Spong[20] discussed application of geometric non-linear control of underactuated mechanical systems and applied to cart pole system, but asymptotic stability is only guaranteed to a manifold and not to a fixed point. M. Yue *et al*.[21] considered dynamic model for a class of two-WMR as the motion of an underactuated vehicle body which can represent the time-varying horizontal distance of the mass center with respect to configuration center. By the computed torque approach, a sliding mode controller with adaptive gain is proposed to overcome the disturbances of system. P. Oryschuk *et al*.[22] reported the implementation and testing of real-time control of an underactuated two-WMR. However, most of the controllers designed for underactuated systems are based on structure and geometry of the systems which are not generalizable. Also, these methods usually do not control all state variables. Mostly, passive variables are ignored or some active variables are added in order to be devoted for passive one.

Tractor–Trailer Wheeled Mobile Robots (TTWMRs) have already been studied in some researches.[23–26] A. K. Khalaji *et al*.[24] proposed a robust adaptive feedback linearizing dynamic controller (RAFLDC) to control a TTWMR using estimated upper-bounds of uncertainties. A. K. Khalaji *et al*.[25] also designed an adaptive dynamic sliding mode controller to control a TTWMR in the presence of external disturbances. A. K. Khalaji *et al*.[26] proposed a non-model based control algorithm using PD-action filtered errors to control a WMR towing two trailers including three non-holonomic constraints. But, in these works, the considered TTWMR is a differential drive wheeled robot with standard wheeled trailers. The fundamental difference of this study is use of spherical wheels in trailer instead of standard wheels in order to increase system maneuverability and degrees of freedom compared to other TTWMRs. Spherical wheels unlike standard wheels which impose pure rolling and non-slip conditions in two directions, provide more maneuverability and degrees of freedom for the system. There is generally an inverse correlation between controllability and maneuverability. For example, the omnidirectional designs such as the four-castor wheel configuration require significant processing to convert desired rotational and translational velocities to individual wheel commands.[1] Due to the change in structure of the robot and use of spherical wheels instead of standard wheels, robot become highly underactuated with severe non-linearities subjected to non-holonomic constraint and makes the robot control more complicated. Trajectory tracking of such complicated TTWMR is a big challenge. To face these complexities, a new controller, i.e. Lyapunov-PID control algorithm, is proposed which contains the following investigations:

- Dynamic modeling of the system including kinetic and kinematic models.
- Introducing and proposing a new control algorithm named Lyapunov-PID control algorithm, as a physical meaningful approach, which can be used for other underactuated systems with the same structure.
- Discussing singularity avoidance in the controller.
- Analyzing stability of the closed loop system.
- Presenting simulation and experimental results in order to show the effectiveness of the proposed method.

2. System Description and Modeling

TTWMR shown in Fig. 1, is a two-wheeled differential drive towing a trailer. Tractor is consisted of two separately actuated standard wheels and a passive spherical wheel is used in order to maintain stability. Standard wheels due to non-slip pure rolling conditions are subjected to non-holonomic constraints, but spherical wheel do not apply any constraint to the system. Tractor is attached to

https://doi.org/10.1017/S0263574716000886 Published online by Cambridge University Press

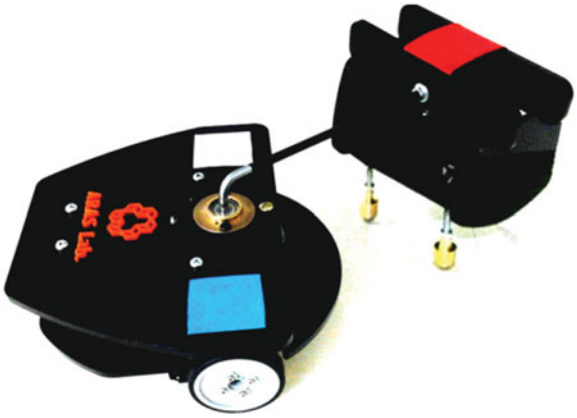

Fig. 1. The robot sample in lab.

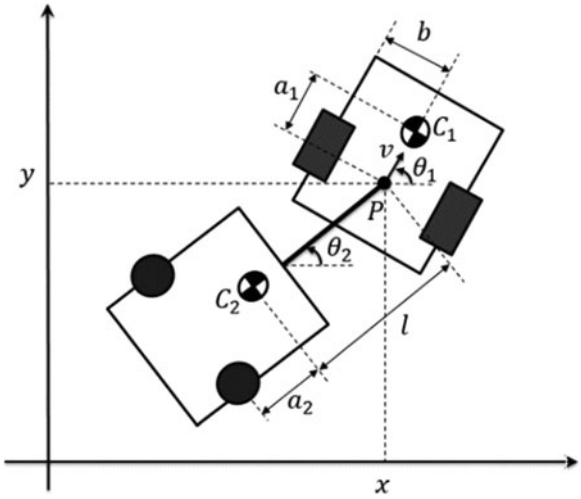

Fig. 2. Structure of wheeled mobile robot attached by a spherical wheeled trailer.

trailer at point P (middle of actuated wheels axis) by a revolute joint. In order to increase system maneuverability, trailer is equipped with two passive spherical wheels. Spherical wheels by rolling in two directions, in addition to increasing system maneuverability and degrees of freedom, do not apply any constraint to the system, but on the other hand makes system highly underactuated.

It is assumed that there is no slip in robot wheels. System motion is considered in a planar environment. System parameters are shown in Fig. 2.

2.1. Kinematic model

The main feature in kinematics of WMRs is the presence of non-holonomic constraints due to non-slip and pure rolling conditions imposed on robot wheels. These non-holonomic constraints can be expressed in Pfaffian form as

$$A(\boldsymbol{q})\,\dot{\boldsymbol{q}} = 0, \tag{1}$$

where $A(\boldsymbol{q})$ is a $(m \times n)$ constraint matrix, where m is the number of constraints, n is the number of generalized coordinates and $\boldsymbol{q}$ is the system generalized coordinates as

$$\boldsymbol{q} = \begin{bmatrix} x & y & \theta_1 & \theta_2 \end{bmatrix}^T. \tag{2}$$

Non-holonomic constraint imposed on tractor wheels is as follows:

$$\dot{x}\sin\theta_1 - \dot{y}\cos\theta_1 = 0. \tag{3}$$

https://doi.org/10.1017/S0263574716000886 Published online by Cambridge University Press

Therefore, the constraint matrix in Pfaffian form can be expressed as

$$A(\boldsymbol{q}) = \begin{bmatrix} \sin\theta_1 & -\cos\theta_1 & 0 & 0 \end{bmatrix}. \tag{4}$$

Note that, from $A\dot{\boldsymbol{q}} = 0$, it can be concluded that there exist a vector $\dot{\boldsymbol{q}}$ spanning the null space of matrix A. Rewriting the relations, the kinematic model of the wheeled robot can be expressed as

$$\dot{\boldsymbol{q}} = S(\boldsymbol{q})\,\dot{\boldsymbol{\zeta}}, \tag{5}$$

where $S(\boldsymbol{q})$ is the jacobian matrix of the system which is a map from system generalized coordinates to workspace variables and this relation can be expressed as

$$\begin{bmatrix} \dot{x} \\ \dot{y} \\ \dot{\theta}_1 \\ \dot{\theta}_2 \end{bmatrix} = \begin{bmatrix} \cos\theta_1 & 0 & 0 \\ \sin\theta_1 & 0 & 0 \\ 0 & 1 & 0 \\ 0 & 0 & 1 \end{bmatrix} \begin{bmatrix} \dot{s} \\ \dot{\theta}_1 \\ \dot{\theta}_2 \end{bmatrix}. \tag{6}$$

Kinematic model inputs are rotational velocities of the tractor wheels (ω_r, ω_l). For simplicity, these kinematic inputs can be transformed to translational speed of point P ($\dot{s}$) and rotational speed of the tractor ($\dot{\theta}_1$) as

$$\boldsymbol{u} = \begin{bmatrix} u_1 & u_2 \end{bmatrix}^{\boldsymbol{T}}, \tag{7}$$

$$u_1 = \frac{r}{2}(\omega_r + \omega_l), \tag{8}$$

$$u_2 = \frac{r}{2b}(\omega_r - \omega_l), \tag{9}$$

where $\boldsymbol{u} = [\,u_1 \quad u_2\,]^{\boldsymbol{T}}$ is the vector of system kinematic control inputs. Now, assuming $u_1 = \dot{s}$ and $u_2 = \dot{\theta}_1$, Eq. (6) can be expressed as follows:

$$\begin{aligned} \dot{x} &= u_1 \cos\theta_1, \\ \dot{y} &= u_1 \sin\theta_1, \\ \dot{\theta}_1 &= u_2, \\ \dot{\theta}_2 &= \dot{\theta}_2. \end{aligned} \tag{10}$$

It is clear that there is no relation between $\dot{\theta}_2$ and other variables or inputs; this is due to the underactuation of the system that has been occurred as a result of using spherical wheels instead of standard wheels in trailer.

2.2. Kinetic model

Lagrange formulation for a constrained system is as

$$\frac{d}{dt}\left(\frac{\partial \mathcal{L}}{d\dot{q}_k}\right) - \left(\frac{\partial \mathcal{L}}{dq_k}\right) = f_k - \sum_{j=1}^{m} \lambda_j a_{jk}, \tag{11}$$

where λ_j is the Lagrange multiplier, m is the number of system constraints, a_{jk} is constraint equations multiplier, f_k is the system generalized force. $\mathcal{L}$ is the Lagrangian of the system, which is the difference between kinetic energy (T) and potential energy (U) of the system as

$$\mathcal{L}(\boldsymbol{q}, \dot{\boldsymbol{q}}) = T(\boldsymbol{q}, \dot{\boldsymbol{q}}) - U(\boldsymbol{q}) = \frac{1}{2}\dot{\boldsymbol{q}}^T B(\boldsymbol{q})\,\dot{q} - U(\boldsymbol{q}), \tag{12}$$

https://doi.org/10.1017/S0263574716000886 Published online by Cambridge University Press

where $B(\boldsymbol{q})$ is the positive definite inertia matrix of the mechanical system. The system kinetic energy is also as follows:

$$T = \frac{1}{2}m_1\left\{\left(\dot{x} - a_1\dot{\theta}_1\sin\theta_1\right)^2 + \left(\dot{y} + a_1\dot{\theta}_1\cos\theta_1\right)^2\right\} + \frac{1}{2}m_2\left\{\left(\dot{x} + l\dot{\theta}_2\sin\theta_2\right)^2 + \left(\dot{y} - l\dot{\theta}_2\cos\theta_2\right)^2\right\} + \frac{1}{2}J_1\dot{\theta}_2^2 + \frac{1}{2}J_2\dot{\theta}_2^2. \tag{13}$$

Since the potential energy is constant, we can consider $\mathcal{L} = T$. The results are as follows:

$$(m_1 + m_2)\,\ddot{x} - m_1a_1\sin\theta_1\ddot{\theta}_1 + m_2l\sin\theta_2\ddot{\theta}_2 - m_1a_1\cos\theta_1\dot{\theta}_1^2 + m_2l\cos\theta_2\dot{\theta}_2^2 = f\cos\theta_1 + \lambda_1\sin\theta_1, \tag{14}$$

$$(m_1 + m_2)\,\ddot{y} + m_1a_1\cos\theta_1\ddot{\theta}_1 - m_2l\cos\theta_2\ddot{\theta}_2 - m_1a_1\sin\theta_1\dot{\theta}_1^2 + m_2l\sin\theta_2\dot{\theta}_2^2 = f\sin\theta_1 - \lambda_1\cos\theta_1, \tag{15}$$

$$m_1a_1\left(-\ddot{x}\,\sin\theta_1 + \ddot{y}\cos\theta_1\right) + \left(J_1 + m_1a_1^2\right)\ddot{\theta}_1 = \tau, \tag{16}$$

$$m_2l\left(\ddot{x}\,\sin\theta_2 - \ddot{y}\cos\theta_2\right) + \left(J_2 + m_2l^2\right)\ddot{\theta}_2 = 0. \tag{17}$$

Therefore, system kinetic equations in matrix form will be as follows:

$$M\left(\boldsymbol{q}\right)\ddot{\boldsymbol{q}} + V\left(\boldsymbol{q},\dot{\boldsymbol{q}}\right) = E\left(\boldsymbol{q}\right)\boldsymbol{\tau} + A^T\left(\boldsymbol{q}\right)\boldsymbol{\lambda}. \tag{18}$$

Using Eqs. (1) and (5), one can write

$$S^T\left(\boldsymbol{q}\right)A^T\left(\boldsymbol{q}\right) = 0. \tag{19}$$

In order to eliminate the constraint forces $A^T(\boldsymbol{q})\boldsymbol{\lambda}$, multiplying the Eq. (18) in Jacobian transpose matrix and using Eq. (19), we can conclude

$$S^T\left(\boldsymbol{q}\right)M\left(\boldsymbol{q}\right)\ddot{\boldsymbol{q}} + S^T\left(\boldsymbol{q}\right)V\left(\boldsymbol{q},\dot{\boldsymbol{q}}\right) = S^T\left(\boldsymbol{q}\right)E\left(\boldsymbol{q}\right)\boldsymbol{\tau}. \tag{20}$$

The first time derivative of Eq. (5) is as

$$\ddot{\boldsymbol{q}} = \dot{S}\left(\boldsymbol{q}\right)\dot{\boldsymbol{\xi}} + S\left(\boldsymbol{q}\right)\ddot{\boldsymbol{\xi}}. \tag{21}$$

Substituting Eq. (21) into Eq. (20), we can conclude

$$S^T\left(\boldsymbol{q}\right)M\left(\boldsymbol{q}\right)\left(\dot{S}\left(\boldsymbol{q}\right)\dot{\boldsymbol{\xi}} + S\left(\boldsymbol{q}\right)\ddot{\boldsymbol{\xi}}\right) + S^T\left(\boldsymbol{q}\right)V\left(\boldsymbol{q},\dot{\boldsymbol{q}}\right) = S^T\left(\boldsymbol{q}\right)E\left(\boldsymbol{q}\right)\boldsymbol{\tau}. \tag{22}$$

Finally, we will have

$$\begin{bmatrix} m_1 + m_2 & 0 & m_2l\sin\left(\theta_2 - \theta_1\right) \\ 0 & J_1 + m_1a_1^2 & 0 \\ m_2l\sin\left(\theta_2 - \theta_1\right) & 0 & J_2 + m_2l^2 \end{bmatrix}\begin{bmatrix} \ddot{s} \\ \ddot{\theta}_1 \\ \ddot{\theta}_2 \end{bmatrix} + \begin{bmatrix} -m_1a_1\dot{\theta}_1^2 + m_2l\cos\left(\theta_2 - \theta_1\right)\dot{\theta}_2^2 \\ m_1a_1\dot{s}\dot{\theta}_1 \\ -m_2l\cos\left(\theta_2 - \theta_1\right)\dot{s}\dot{\theta}_1 \end{bmatrix} = \begin{bmatrix} f \\ \tau \\ 0 \end{bmatrix}. \tag{23}$$

Underactuation of the system is also evident in kinetics equations.

https://doi.org/10.1017/S0263574716000886 Published online by Cambridge University Press

2.3. Hybrid model

Control of WMRs has been mostly focused on kinematic control algorithms. However, the lack of adequate information and relationships as well as the lack of appropriate control algorithms for underactuated systems provide some difficulties relating to control of these systems based on kinetic and kinematic algorithms. Therefore, it is important to have an appropriate modeling order to introduce the system dynamics correctly. To this end, a hybrid dynamics model is derived for the system, combining kinematics and kinetics equations. Due to the underactuated nature of the system, orientation of the trailer (θ_2) cannot be calculated using system kinematic equations. For this system, tractor is subjected to a first-order non-holonomic constraint and its position can be obtained from kinematic equations in any instant of time. Note that the trailer has no kinematic constraint; its kinetic equation is used as a second-order non-holonomic constraint in order to solve system equations. In fact, we have an underactuated system with four degrees of freedom subjected to a first-order non-holonomic constraint and a second-order non-holonomic constraint. To this end, Eq. (17) is added to Eq. (10).

$$\begin{aligned}
&\dot{x} = u_1 \cos\theta_1, \\
&\dot{y} = u_1 \sin\theta_1, \\
&\dot{\theta}_1 = u_2, \\
&\dot{\theta}_2 = \dot{\theta}_2, \\
&\ddot{x}\ \sin\theta_2 - \ddot{y}\cos\theta_2 + k\ddot{\theta}_2 = 0,
\end{aligned} \tag{24}$$

where k is as

$$k = J_2/m_2 l + l$$

Unlike conventional methods for the control of WMRs, which θ_1 is considered as one of the system generalized coordinates, $\dot{x}$ and $\dot{y}$ are added to the generalized coordinates. The systems state variables is as

$$z = \left[x, \dot{x}, y, \dot{y}, \theta_2, \dot{\theta}_2\right]^T. \tag{25}$$

Therefore, we will have

$$\begin{aligned}
&\dot{z}_1 = \dot{x} = z_2, \\
&\dot{z}_2 = \ddot{x} = \dot{u}_1 \cos\theta_1 - u_1 u_2 \sin\theta_1, \\
&\dot{z}_3 = \dot{y} = z_4, \\
&\dot{z}_4 = \ddot{y} = \dot{u}_1 \sin\theta_1 + u_1 u_2 \cos\theta_1, \\
&\dot{z}_5 = \dot{\theta}_2 = z_6, \\
&\dot{z}_6 = \ddot{\theta}_2 = \left(-\ddot{x}\ \sin z_5 + \ddot{y}\ \cos z_5\right)/k.
\end{aligned} \tag{26}$$

Now the following transformations have been considered for system input variables:

$$v_1 = \dot{u}_1 \cos\theta_1 - u_1 u_2 \sin\theta_1, \tag{27}$$

$$v_2 = \dot{u}_1 \sin\theta_1 + u_1 u_2 \cos\theta_1. \tag{28}$$

So, the following state space equations are resulted for the system.

$$\begin{aligned}
&\dot{z}_1 = z_2, \\
&\dot{z}_2 = v_1, \\
&\dot{z}_3 = z_4, \\
&\dot{z}_4 = v_2, \\
&\dot{z}_5 = z_6, \\
&\dot{z}_6 = \left(-v_1 \sin z_5 + v_2 \cos z_5\right)/k.
\end{aligned} \tag{29}$$

https://doi.org/10.1017/S0263574716000886 Published online by Cambridge University Press

3. Control Algorithm Design

Mobile robots controllers can be divided into two groups. Some of the control algorithms are proposed for kinematic models which their inputs are velocities. Others are proposed for kinetic models which their inputs are forces and torques. Control of WMRs has been proposed mainly based on kinematic control. Major reasons are as follows:

- Kinematic models are simpler than kinetic models.
- Most of mobile robots' actuators are servo motors. These motors often have velocity control loops with rotational velocity inputs.
- Problems with actuators' torques control can be changed to a problem with accelerate control inputs.

In fact, obtaining the hybrid model is due to system underactuation. So, kinetic equation of trailer orientation which is a second-order non-holonomic constraint is added to kinematic equations. Now, the aim is to control an underactuated system with a first-order non-holonomic constraint and a second-order non-holonomic constraint. In the following, based on a physical intuition, a new controller is developed for the robot, i.e. Lyapaunov-PID control algorithm.

One of most common ways to control a two-WMR is to design control laws based on Lyapunov method. As mentioned, there is no kinematic relation between the orientation of the trailer and other variables. Therefore, at first, it is tried to control the tractor, while ignoring the orientation of the trailer. In fact, controlling the active variables (position and orientation of the tractor) is the aim. In this situation, there is no control on the trailer and because of attachment to the tractor, has an unknown motion.

3.1. Physical description of the controller

In this section, first control of tractor is focused and a control algorithm is designed based on Lyapunov method. Then, based on this intuition, a torsion spring and damper is added at point P to control all the system.

3.1.1. Controlling the tractor. The concept of a Lyapunov function originates from theoretical mechanics. Here, we see that in stable conservative systems "energy" is a positive definite scalar function which should decrease with time. Using this analogy, we can define a generalized energy as a Lyapunov function to analyze stability for any non-linear system.[27] Here, a Lyapunov function candidate which consists of tractors' variables is proposed. The aim is to derive a control law to control the tractor. The following tracking errors are defined:

$$\begin{cases} e_1 = x - x_d = z_1 - z_{1d} \\ e_2 = \dot{x} - \dot{x}_d = z_2 - z_{2d} \\ e_3 = y - y_d = z_3 - z_{3d} \\ e_4 = \dot{y} - \dot{y}_d = z_4 - z_{4d} \end{cases}. \tag{30}$$

Substituting first time derivative of Eq. (30) into Eq. (29) yields

$$\begin{aligned} \dot{e}_1 &= e_2, \\ \dot{e}_2 &= v_1 - v_{1d}, \\ \dot{e}_3 &= e_4, \\ \dot{e}_4 &= v_2 - v_{2d}, \\ \dot{z}_5 &= z_6, \\ \dot{z}_6 &= \left(-v_1 \sin z_5 + v_2 \cos z_5\right)/k. \end{aligned} \tag{31}$$

Now consider the following control inputs:

$$\begin{cases} v_1 = v_{1d} - \alpha_2 e_2 - \frac{\alpha_1}{\alpha_2}\left(e_1 + \frac{e_1^2}{e_2}\right) \\ v_2 = v_{2d} - \alpha_4 e_4 - \frac{\alpha_3}{\alpha_4}\left(e_3 + \frac{e_3^2}{e_4}\right) \end{cases}. \tag{32}$$

https://doi.org/10.1017/S0263574716000886 Published online by Cambridge University Press

Table I. System parameters.

Parameters	Descriptions	Value
m_1 (kg)	Mass of the tractor	0.9
m_2 (kg)	Mass of the trailer	0.33
J_1 (kg.m^2)	Mass moment of inertia of the tractor	0.0035
J_2 (kg.m^2)	Mass moment of inertia of the trailer	0.00078
a_1 (m)	Length of PC_1	0.029
l (m)	Length of PC_2	0.141
r (m)	Radius of tractor wheels	0.026
$2b$ (m)	Distance between tractor wheels	0.1190

Theorem 1. The control law (32) guarantees asymptotic stabilization of the dynamic system described by Eq. (31) to the origin as $t \to \infty$.

Proof : To ensure the asymptotic stabilization, the following Lyapunov function candidate is proposed:

$$\begin{array}{l} V(e) = \frac{1}{2}\left(\alpha_1 e_1^2 + \alpha_2 e_2^2 + \alpha_3 e_3^2 + \alpha_4 e_4^2\right) \\ \alpha_1, \alpha_2, \alpha_3, \alpha_4 > 0. \end{array} \tag{33}$$

The first derivative of the chosen Lyapunov function candidate is as

$$\dot{V}(e) = \left(\alpha_1 e_1 \dot{e}_1 + \alpha_2 e_2 \dot{e}_2 + \alpha_3 e_3 \dot{e}_3 + \alpha_4 e_4 \dot{e}_4\right). \tag{34}$$

Substitution from Eq. (31) into Eq. (34) yields

$$\dot{V}(e) = \alpha_1 e_1 e_2 + \alpha_2 e_2 (v_1 - v_{1d}) + \alpha_3 e_3 e_4 + \alpha_4 e_4 (v_2 - v_{2d}). \tag{35}$$

Substitution from Eq. (32) into the derivative of the Lyapunov function candidate will have

$$\dot{V}(e) = -\alpha_1 e_1^2 - (\alpha_2 e_2)^2 - \alpha_3 e_3^2 - (\alpha_4 e_4)^2. \tag{36}$$

It's evident from Eq. (36) that the derivative of the Lyapunov function candidate is a negative definite function. Therefore, the chosen tracking errors will be asymptotically stable.

3.1.1.1. Simulation results. Now, the proposed algorithm is simulated on the following circular trajectory. System parameters are given in Table I.

$$\begin{array}{l} x = r\cos(\omega t), \\ y = r\sin(\omega t). \end{array} \tag{37}$$

The results are (for $r = 1,\ \omega = 0.5$) shown in Figs. 3 and 4.

As can be seen from Fig. 3, tractor has followed the desired trajectory appropriately. But as it can be seen from Fig. 4, the trailer oscillates around the reference trajectory and this is because of that there is no control on the trailer. To handle this problem and eliminate vibrations, a torsion spring and damper is considered to attach in point P (in connection point of tractor and trailer).

3.1.2. Adding torsion spring and damper. In this section, a torsion spring and damper is added in point P, attachment point of trailer to tractor. Therefore, Eq. (17) should be retrieved in order to contain the influence of adding torsion spring and damper. Note that adding spring and damper do not change the kinetic energy of the system and it will be the same as Eq. (13). In this case, general Lagrange formulation has been used which is as follows:

$$\frac{d}{dt}\left(\frac{\partial \mathcal{L}}{d\dot{q}_k}\right) - \left(\frac{\partial \mathcal{L}}{dq_k}\right) + \frac{\partial F}{d\dot{q}_k} = f_k - \sum_{j=1}^{m} \lambda_j a_{jk}, \tag{38}$$

https://doi.org/10.1017/S0263574716000886 Published online by Cambridge University Press

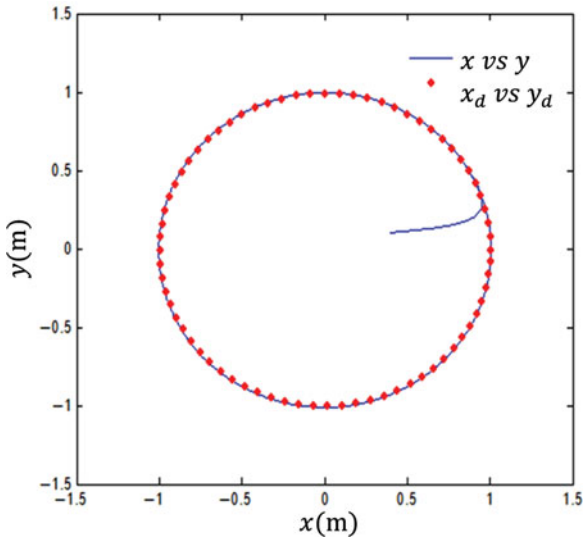

Fig. 3. Tracking desired trajectories in cartesian space for the tractor.

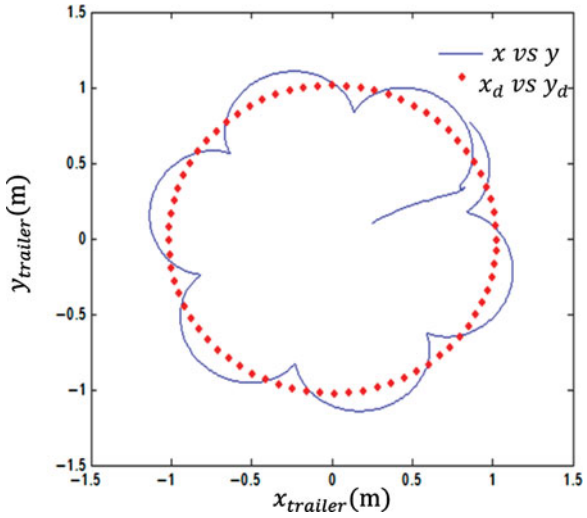

Fig. 4. Tracking desired trajectories in cartesian space for the trailer.

where the dampers term (F) and potential energy of the system (U) can be obtained as follows:

$$U = \frac{1}{2}k_t(\theta_1 - \theta_2)^2, \tag{39}$$

$$F = \frac{1}{2}\sum_{r=1}^{n}\sum_{s=1}^{n} c_{rs}\dot{q}_r\dot{q}_s = \frac{1}{2}c_t\left(\dot{\theta}_1 - \dot{\theta}_2\right)^2. \tag{40}$$

Therefore, we will have

$$\ddot{\theta}_2 = \frac{1}{k}\left(-\ddot{x}\sin\theta_2 + \ddot{y}\cos\theta_2 + k_t\left(\theta_1 - \theta_2\right) + c_t\left(\dot{\theta}_1 - \dot{\theta}_2\right)\right), \tag{41}$$

$$\dot{z}_6 = \frac{1}{k}\left(-v_1\sin z_5 + v_2\cos z_5 + k_t\left(\theta_1 - \theta_2\right) + c_t\left(\dot{\theta}_1 - \dot{\theta}_2\right)\right). \tag{42}$$

https://doi.org/10.1017/S0263574716000886 Published online by Cambridge University Press

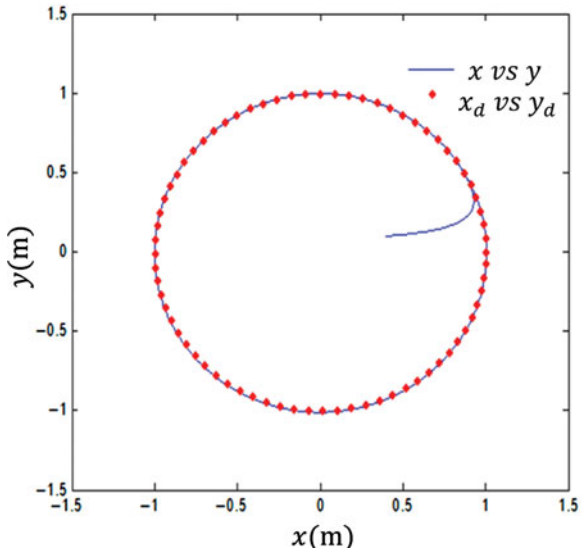

Fig. 5. Tracking desired trajectories in cartesian space for the tractor in presence of torsion spring and damper at point P.

Substituting Eq. (42) instead of the last relation in Eq. (31) yields

$$\begin{aligned}
\dot{e}_1 &= e_2,\\
\dot{e}_2 &= v_1 - v_{1d},\\
\dot{e}_3 &= e_4,\\
\dot{e}_4 &= v_2 - v_{2d},\\
\dot{z}_5 &= z_6,\\
\dot{z}_6 &= \tfrac{1}{k}\left(-v_1 \sin z_5 + v_2 \cos z_5 + k_t\left(\theta_1 - \theta_2\right) + c_t\left(\dot{\theta}_1 - \dot{\theta}_2\right)\right).
\end{aligned} \tag{43}$$

Theorem 2. With the designed control law (32), tracking error signals, for the dynamic system (31), will asymptotically converge to zero.

Proof : Consider the following Lyapunov function candidate:

$$\begin{aligned}
&V\left(e\right) = \tfrac{1}{2}\left(\alpha_1 e_1^2 + \alpha_2 e_2^2 + \alpha_3 e_3^2 + \alpha_4 e_4^2\right)\\
&\alpha_1, \alpha_2, \alpha_3, \alpha_4 > 0.
\end{aligned} \tag{44}$$

The first derivative of the chosen Lyapunov function candidate is as

$$\dot{V}\left(e\right) = \left(\alpha_1 e_1 \dot{e}_1 + \alpha_2 e_2 \dot{e}_2 + \alpha_3 e_3 \dot{e}_3 + \alpha_4 e_4 \dot{e}_4\right). \tag{45}$$

Substitution from Eqs. (32) and (42) into Eq. (45), yields

$$\dot{V}\left(e\right) = -\alpha_1 e_1^2 - \left(\alpha_2 e_2\right)^2 - \alpha_3 e_3^2 - \left(\alpha_4 e_4\right)^2. \tag{46}$$

It's evident from Eq. (46) that the derivative of the Lyapunov function candidate is a negative definite function. Therefore, the chosen tracking errors will be asymptotically stable.

3.1.2.1. Simulation results. Now simulation is done for a circular trajectory given in Eq. (37). The results are shown in Figs. 5 and 6, where controller parameters are given in Table II.

Obtained results reveals that adding torsion spring and damper is an appropriate solution for the oscillations of the trailer and the system is completely controlled. Note that, the considered spring and damper can be used virtually through control algorithm. Therefore, designed controller should be modified in order to play the roles of torsion spring and damper by its own. In the next section, we will focus on this issue.

https://doi.org/10.1017/S0263574716000886 Published online by Cambridge University Press

Table II. Controller parameters.

Parameters	Value
α_1, α_3	25
α_2, α_4	10
k_t (N/m)	200
c_t (N.s/m)	200
ρ	2.5
k_d	12
k_p	48
k_i	64
(x_0, y_0)	(0.6, −0.3)

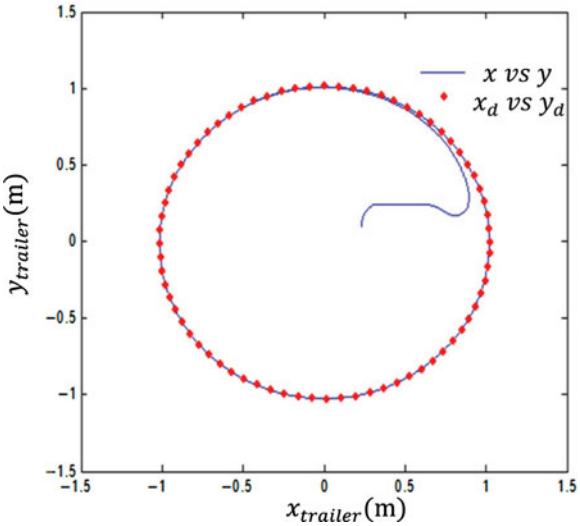

Fig. 6. Tracking desired trajectories in cartesian space for the trailer in presence of torsion spring and damper at point P.

3.2. Lyapunov-PID control algorithm

As mentioned, now the effort is on modifying the designed control algorithm, in addition to the control of the tractor, the control algorithm should also act as torsion spring and damper at point P. To this end, following control law is proposed:

$$\begin{cases} \bar{v}_1 = v_{1d} - \alpha_2 e_2 - \frac{\alpha_1}{\alpha_2}\left(e_1 + \frac{e_1^2}{e_2}\right) + \alpha_4 e_4 \gamma \\ \bar{v}_2 = v_{2d} - \alpha_4 e_4 - \frac{\alpha_3}{\alpha_4}\left(e_3 + \frac{e_3^2}{e_4}\right) - \alpha_2 e_2 \gamma \end{cases}, \tag{47}$$

where γ is defined as

$$\gamma = \frac{1}{\alpha_4 e_4 \sin\theta_2 + \alpha_2 e_2 \cos\theta_2} \times \left\{(-v_1 \sin\theta_2 + v_2 \cos\theta_2) - k\left(\ddot{\theta}_{2d} + k_d\left(\dot{\theta}_{2d} - \dot{\theta}_2\right) + k_p\left(\theta_{2d} - \theta_2\right) + k_i \int (\theta_{2d} - \theta_2)\, dt\right)\right\}. \tag{48}$$

Theorem 3. The control law (47) guarantees asymptotic stabilization of the dynamic system described by Eq. (31) to the origin as $t \to \infty$.

https://doi.org/10.1017/S0263574716000886 Published online by Cambridge University Press

Proof : Designed control algorithm (32) should be modified in order to act as a torsion spring and damper. To this end, the same Lyapunov function candidate (33) is proposed. Then, two corrective terms is added to the designed inputs (32). Note that these corrective terms should be obtained in order that the closed loop system still remains stable. In fact, corrective terms are added to control the orientation of the trailer as a torsion spring and damper. In other words, corrective terms are added as a virtual spring and damper. Therefore, modified control inputs are as follows:

$$\begin{cases} \bar{v}_1 = v_1 + \beta_1\gamma_1 \\ \bar{v}_2 = v_2 + \beta_2\gamma_2 \end{cases}, \tag{49}$$

where $\beta_1\gamma_1$ and $\beta_2\gamma_2$ are corrective terms. In addition to not effecting stability of the closed loop system and controlling of the tractor, corrective terms must and act as a virtual spring and damper at joint P in order to control the trailer. Substituting the new control inputs (49) into the derivative of candidate Lyapunov function (34) yields

$$\dot{V}(e) = \alpha_1 e_1 e_2 + \alpha_2 e_2 (\bar{v}_1 - v_{1d}) + \alpha_3 e_3 e_4 + \alpha_4 e_4 (\bar{v}_2 - v_{2d}). \tag{50}$$

Substituting from Eq. (49) into (50) yields

$$\dot{V}(e) = \alpha_1 e_1 e_2 + \alpha_2 e_2 (v_1 + \beta_1\gamma_1 - v_{1d}) + \alpha_3 e_3 e_4 + \alpha_4 e_4 (v_2 + \beta_2\gamma_2 - v_{2d}). \tag{51}$$

Substitution v_1 and v_2 from Eq. (32) into (51) and simplifications yield

$$\dot{V}(e) = -\alpha_1 e_1^2 - (\alpha_2 e_2)^2 - \alpha_3 e_3^2 - (\alpha_4 e_4)^2 + \alpha_2 e_2 \beta_1 \gamma_1 + \alpha_4 e_4 \beta_2 \gamma_2 < 0. \tag{52}$$

The idea is to eliminate the effects of the new terms appeared in Eq. (52) comparing to Eq. (36) due to adding corrective terms. Therefore, we assume

$$\alpha_2 e_2 \beta_1 \gamma_1 + \alpha_4 e_4 \beta_2 \gamma_2 = 0. \tag{53}$$

In order to fulfill Eq. (53), the following choices have been considered:

$$\begin{cases} \beta_1 = +\alpha_4 e_4 \\ \beta_2 = -\alpha_2 e_2 \\ \gamma_1 = \gamma_2 = \gamma \end{cases}. \tag{54}$$

Substituting Eq. (54) into Eq. (49) yields

$$\begin{cases} \bar{v}_1 = v_1 + \alpha_4 e_4 \gamma \\ \bar{v}_2 = v_2 - \alpha_2 e_2 \gamma \end{cases}. \tag{55}$$

Now γ in Eq. (55) should be determined. To this end, the control inputs (55) are substituted in the last equation of the state space Eq. (31) as

$$\dot{z}_6 = (-\bar{v}_1 \sin z_5 + \bar{v}_2 \cos z_5)/k. \tag{56}$$

Note that $\dot{z}_6 = \ddot{\theta}_2$, therefore

$$\ddot{\theta}_2 = \frac{1}{k}(-(v_1 + \alpha_4 e_4 \gamma)\sin\theta_2 + (v_2 - \alpha_2 e_2 \gamma)\cos\theta_2). \tag{57}$$

Simplifications yield

$$\ddot{\theta}_2 = \frac{1}{k}\{(-v_1 \sin\theta_2 + v_2 \cos\theta_2) + (\alpha_4 e_4 \sin\theta_2 + \alpha_2 e_2 \cos\theta_2)\gamma\}. \tag{58}$$

https://doi.org/10.1017/S0263574716000886 Published online by Cambridge University Press

Comparing Eq. (58) with Eq. (41), and noting that the corrective terms must act like a spring and damper, it can be concluded that

$$-\left(\alpha_4 e_4 \sin\theta_2 + \alpha_2 e_2 \cos\theta_2\right)\gamma = k_t\left(\theta_1 - \theta_2\right) + c_t\left(\dot{\theta}_1 - \dot{\theta}_2\right). \tag{59}$$

Therefore, γ can be obtained as follows:

$$\gamma = -\frac{k_t\left(\theta_1 - \theta_2\right) + c_t\left(\dot{\theta}_1 - \dot{\theta}_2\right)}{\left(\alpha_4 e_4 \sin\theta_2 + \alpha_2 e_2 \cos\theta_2\right)}. \tag{60}$$

We can use feedback linearization technique in Eq. (58), therefore γ can be obtained as follows:

$$\gamma = \frac{1}{\alpha_4 e_4 \sin\theta_2 + \alpha_2 e_2 \cos\theta_2} \times \left\{\left(-v_1 \sin\theta_2 + v_2 \cos\theta_2\right) - k\left(\ddot{\theta}_{2d} + k_d\left(\dot{\theta}_{2d} - \dot{\theta}_2\right) + k_p\left(\theta_{2d} - \theta_2\right) + k_i \int \left(\theta_{2d} - \theta_2\right)\, \mathrm{d}t\right)\right\}. \tag{61}$$

Now PID-action gains should be obtained. In order to do this, substitution Eq. (61) into Eq. (58) and simplifications yield

$$\ddot{\theta}_2 = \ddot{\theta}_{2d} + k_d\left(\dot{\theta}_{2d} - \dot{\theta}_2\right) + k_p\left(\theta_{2d} - \theta_2\right) + k_i \int \left(\theta_{2d} - \theta_2\right) \mathrm{d}t. \tag{62}$$

The error signal for θ_2 is as follows:

$$e_5(t) = \theta_2 - \theta_{2d}. \tag{63}$$

Therefore, substitution from Eq. (63) into Eq. (62) leads to

$$\ddot{e}_5 + k_d \dot{e}_5 + k_p e_5 + k_i \int e_5\, \mathrm{d}t = 0. \tag{64}$$

By taking the Laplace transform of Eq. (64), we will have

$$E_5(s)\left(s^3 + k_d s^2 + k_p s + k_i\right) = 0. \tag{65}$$

Now using pole placement, for example in -1, controller gains will be obtained as

$$(s+1)^3 = s^3 + 3s^2 + 3s + 1 = 0, \tag{66}$$

$$\begin{cases} k_d = 3 \\ k_p = 3 \\ k_i = 1 \end{cases}. \tag{67}$$

3.3. Singularity avoidance of the controller

In order to avoid the closed loop system from singularity, some modifications have been considered. The main reason for singularity of the system is the errors in the denominator of the Eq. (48). If the errors go toward zero, the expression (48) will tend to infinity.

Since the error values are in the vicinity of zero and have small variations, the following approximation can be considered:

$$\alpha_4 e_4 \sin e_5 + \alpha_2 e_2 \cos e_5 = const + \varepsilon. \tag{68}$$

https://doi.org/10.1017/S0263574716000886 Published online by Cambridge University Press

The value of ε is negligible, therefore it can be ignored. Since the small value is located in the denominator, it generates a large amount; this great value is also considered to be a constant.

$$\frac{1}{\alpha_4 e_4 \sin e_5 + \alpha_2 e_2 \cos e_5} = \frac{1}{const + \varepsilon} = \rho. \tag{69}$$

In other words, the control inputs are as follows:

$$\begin{cases} \bar{v}_1 = v_{1d} - \alpha_2 e_2 - \frac{\alpha_1}{\alpha_2}\left(e_1 + \frac{e_1^2}{e_2}\right) + \alpha_4 e_4 \gamma \\ \bar{v}_2 = v_{2d} - \alpha_4 e_4 - \frac{\alpha_3}{\alpha_4}\left(e_3 + \frac{e_3^2}{e_4}\right) - \alpha_2 e_2 \gamma \end{cases}, \tag{70}$$

where γ is defined as

$$\gamma = \rho\left[(-v_1 \sin\theta_2 + v_2 \cos\theta_2) - k\left(\ddot{\theta}_{2d} + k_d\left(\dot{\theta}_{2d} - \dot{\theta}_2\right) + k_p\left(\theta_{2d} - \theta_2\right) + k_i \int \left(\theta_{2d} - \theta_2\right)\, \mathrm{d}t\right)\right], \tag{71}$$

where ρ is a constant value.

3.4. Simulation results

In this section, obtained results for tracking of the reference trajectories are shown in Figs. 7 and 8. A circular path in Cartesian space with a specified timing law is used as the reference trajectories which is defined as

$$x_d = 0.43 \cos\left(\frac{t}{8} + 0.35\right), \tag{72}$$

$$y_d = 0.43 \sin\left(\frac{t}{8} + 0.35\right). \tag{73}$$

Controller parameters are given in Table II. System controller gains have the same values both in simulation and experimental results. Positive values for controller gains support system closed loop stability, but in order to avoid unreasonable control inputs and also having appropriate performance of the closed loop system, they have selected using simulation studies. Higher controller gains lead to higher control inputs and better performance of the closed loop system; however, lower controller gains results in lower control inputs and degraded performance of the closed loop system (oscillating responses, higher settling times, overshoot, and so on). These gains have been tuned manually using trial and error method through simulations and simultaneously checking the control inputs and performance of the closed loop system.

Obtained simulation results reveal the performance of the designed controller. Both tractor and trailer has tracked desired trajectories (Figs. 7 and 8) appropriately. Therefore, next step is the experimental implementation of the proposed approach.

4. Experimental Implementation

In this section, implementation and experimental results are presented.

As shown in Figs. 1 and 9, Colored labels were used to provide the position and orientations of the TTWMR for tracking reference trajectory. DC servo motors are used as system actuators which are mounted on the wheels of the tractor. DC servo-motors have 1.62 N.m holding torque, and 12 V operating voltage. The servo motors are controlled by the PWM signals. An I/O card is employed to generate PWM signals, and to drive the DC servo motors. A real-time image processing module estimates the posture information of the TTWMR by installing a camera above the motion plane; Fig. 9, and transmits it to the host computer. This module consists of a camera with resolution of 640 × 480 pixels. Since the localization of the robot is made only by the vision system, the processing rate of the vision system limits the sampling time for the controller. In the experiments, the sampling time is set to be 33 ms, which is identical to the processing rate. An image taken by the camera in gray

https://doi.org/10.1017/S0263574716000886 Published online by Cambridge University Press

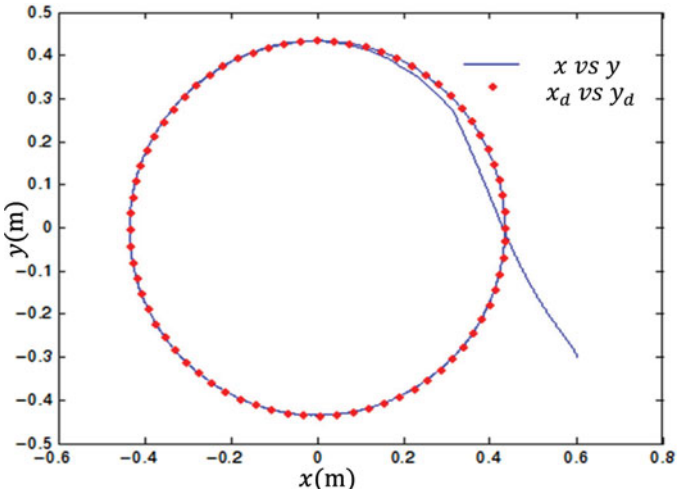

Fig. 7. Tracking desired trajectories in cartesian space for the tractor (simulation result with Lyapunov-PID controller).

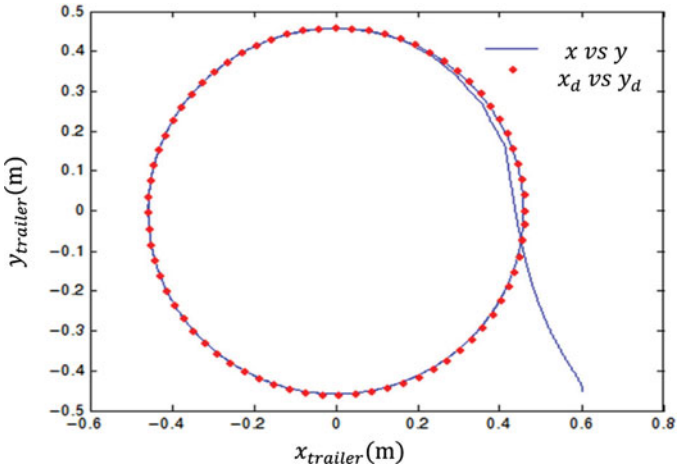

Fig. 8. Tracking desired trajectories in cartesian space for the trailer (simulation result with Lyapunov-PID controller).

scale is shown in Fig. 10. The host computer is using an Intel Core i5, 3.60GHz processor. Control commands are generated from the host computer and sent to the robot through the communication system, which is a cable with USB connections. Here is the list of some necessary compensations have been done in order to obtain higher precisions.

- **Image acquisition Device** – Digital image is produced by a camera with 30 frame/second frame rate. The frame rate of the camera is an important factor in precision of the real time image processing module.
- **Camera Calibration** – In order to estimate the position of a specific colored label relative to an inertial frame camera calibration is performed.
- **Image restoration** – The aim of image restoration is the removal of noise (sensor noise, motion blur, etc.) from images. The simplest possible approach for noise removal is various types of filters. Image restoration is used in order to remove colored areas larger or smaller than colored labels.
- **Detection** – Detection of colored labels is performed based on relatively simple and fast computations for finding a specific colored label around multiple expected image regions to produce a correct result.
- **Tracking** – Following the movements of colored points in the image sequence.

https://doi.org/10.1017/S0263574716000886 Published online by Cambridge University Press

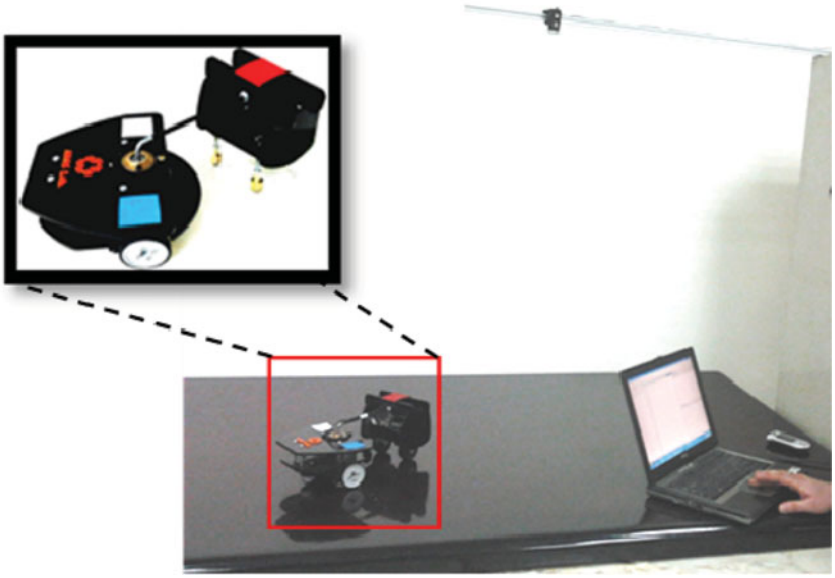

Fig. 9. Experimental setup.

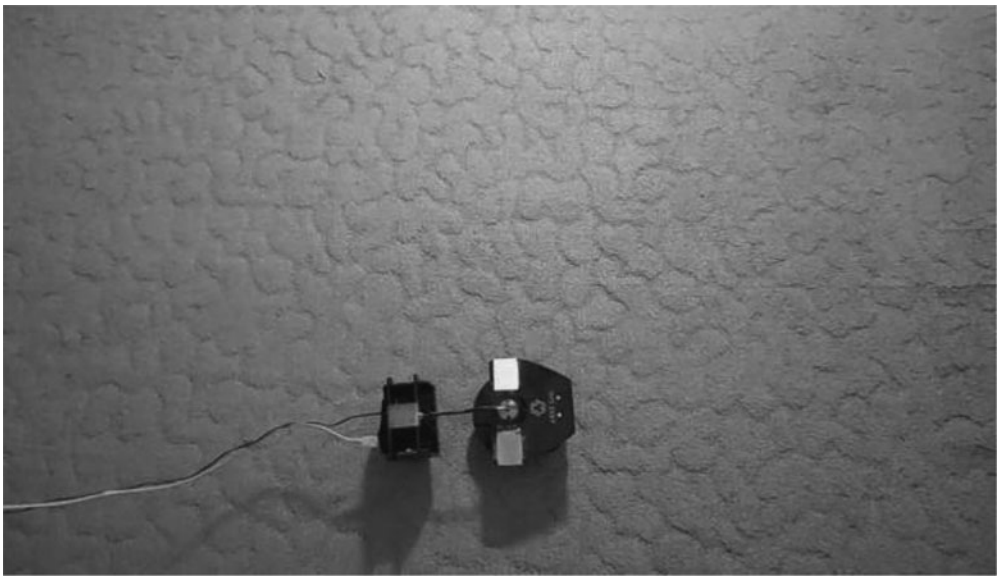

Fig. 10. Gray scale image taken by camera.

In order to increase the speed of image processing algorithm, MEX-file is used in MATLAB/Simulink environment.

A circular path in Cartesian space with a specified timing law is used as reference trajectories which is the same as simulation path (72) and (73). Experimental implementation results verify the simulation results and performance of Lyapunov-PID control algorithm. Implementation results are shown in Figs. 11-18. In Figs. 11 and 12, tractor and trailer start tracking desired trajectories in Cartesian space from initial condition.

As can be seen from obtained results (in Figs. 11 and 12), tractor and trailer tracked the trajectories appropriately, similar to the simulation results. In order to analyze the behavior of the system, tracking results for each coordinate is shown separately in Figs. 13–16.

In Fig. 19, tracking of an 8 type trajectory using the proposed control algorithm can also be seen.

https://doi.org/10.1017/S0263574716000886 Published online by Cambridge University Press

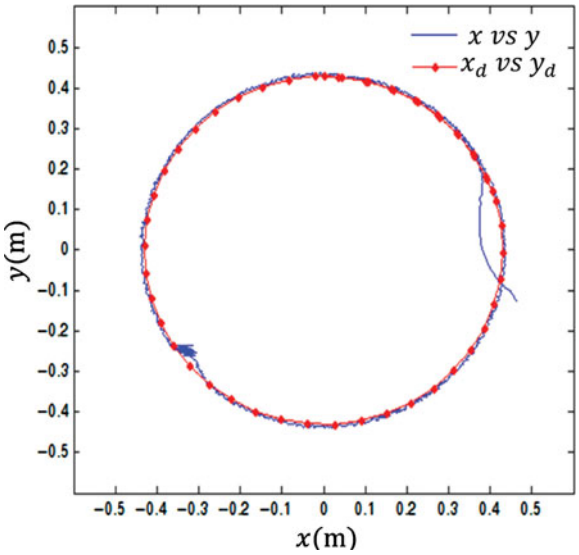

Fig. 11. Tracking desired trajectories in cartesian space for the tractor; experimental implementation results.

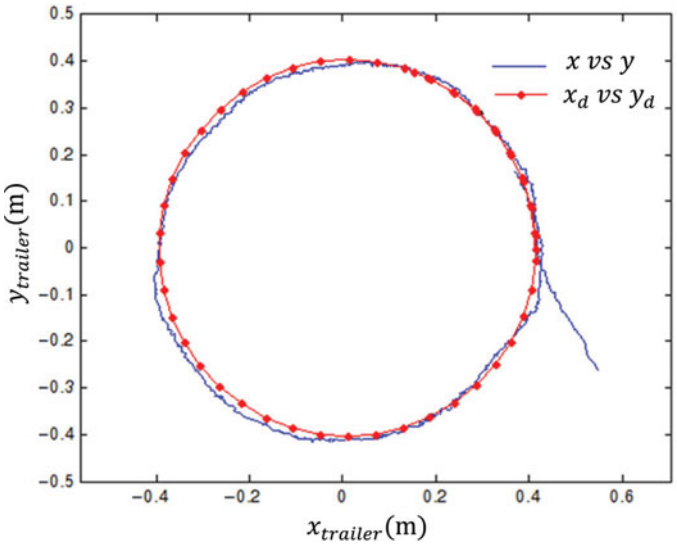

Fig. 12. Tracking desired trajectories in cartesian space for the trailer; experimental implementation results.

Obtained results show that all generalized coordinates track reference trajectories appropriately. In Figs. 17 and 18, kinematic inputs are shown. Kinematic inputs are angular velocities of tractor wheels, which are produced by actuators (servo motors).

As can be seen, experimental and simulated results are in reasonable agreement. The basic trends in experimental results are similar to those predicted by theoretical simulations. Only, some deviations from the reference signals also exist in the experimental results which is realistic due to the external disturbances, uncertainties and other unknown and unpredictable features exist in real systems. The proposed algorithm reveals the characteristic of finite-time convergence of tracking errors under the effects of unpredictable uncertainties in real systems. As it can be seen, the system follows the desired reference path with very low efforts of actuators. It is seen that tracking of reference trajectories is effectively achieved using the proposed method. Obtained results indicate that the proposed algorithm is remarkably effective, which may be employed for other non-holonomic underactuated systems.

Some of the future works of this study include control of multiple trailer systems similar to the snake-like robots in order to evaluate the agility of the system in different maneuvers or clumsy environments. Control of such a system is a challenging problem that needs more investigations, and

https://doi.org/10.1017/S0263574716000886 Published online by Cambridge University Press

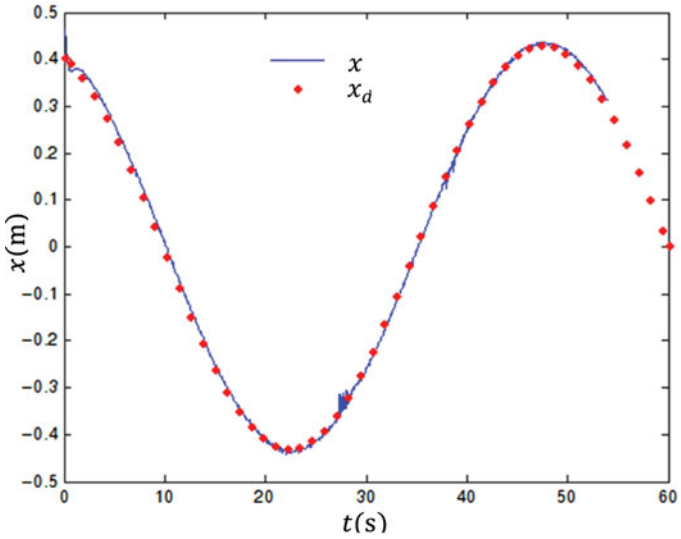

Fig. 13. Trajectory tracking for x variable of the location of the tractor; experimental implementation results.

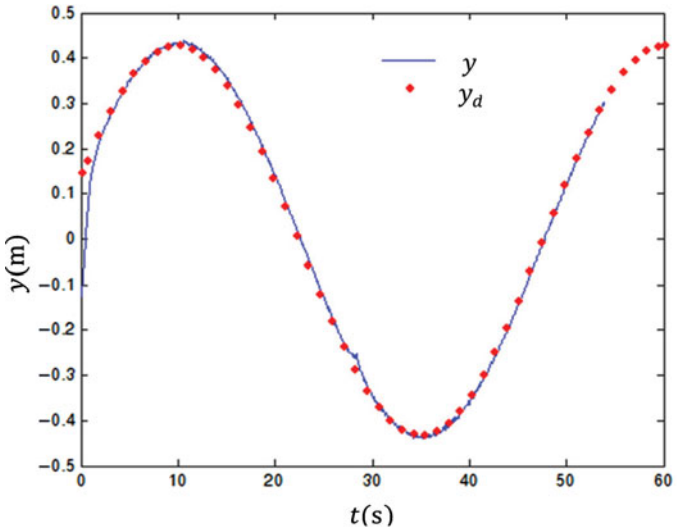

Fig. 14. Trajectory tracking for y variable of the location of the tractor; experimental implementation results.

makes the trend of our future works. Implementations in outdoor wheeled vehicles and proposing controllers with better capabilities are also the next future works of this study.

Existence of first- and second-order non-holonomic constraints could also arise in different engineering systems (such as underwater vehicles, free floating spatial systems, robotic manipulators and so on) that obtained results in this study could be also helpful for those applications.

5. Conclusions

In this paper, the problem of controlling a TTWMR consisted of a differential drive wheeled robot towing a spherical wheeled trailer, as a highly underactuated system with severe non-linearities with non-holonomic constraints, was discussed. First, the robot was introduced and the structure of the system was described. Next kinematics and kinetics models, were combined. Then, based on a physical intuition a new controller was developed for the robot as Lyapunov-PID control algorithm. Subsequently, singularity avoidance and stability of the system were analyzed. Finally, simulation and experimental implementation results revealed the effectiveness of the proposed algorithm.

https://doi.org/10.1017/S0263574716000886 Published online by Cambridge University Press

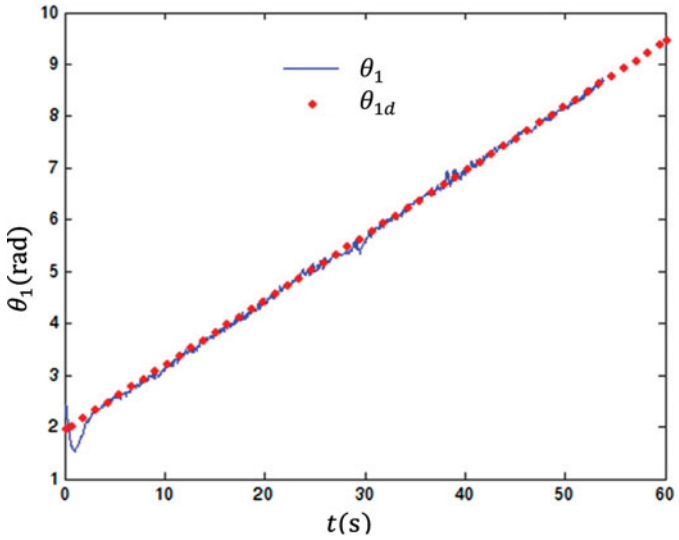

Fig. 15. Trajectory tracking for θ_1 variable, orientation of the tractor; experimental implementation results.

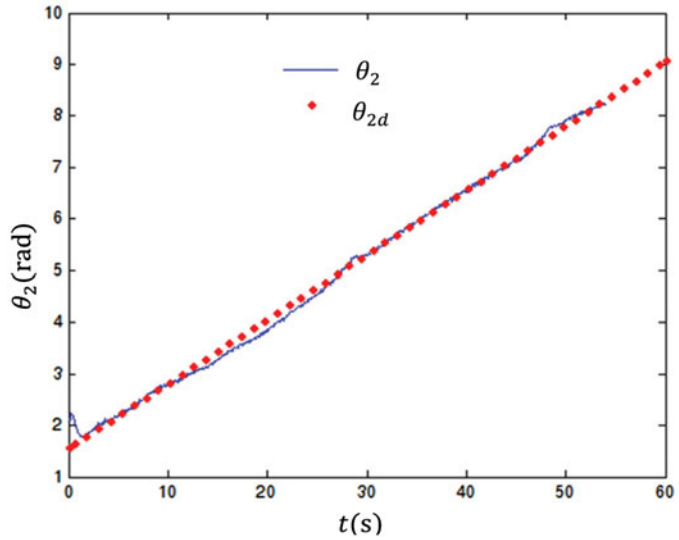

Fig. 16. Trajectory tracking for θ_2 variable, orientation of the trailer; experimental implementation results.

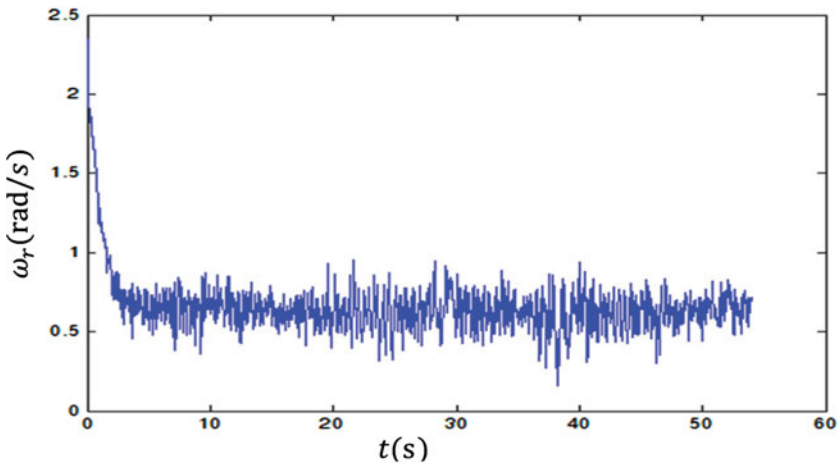

Fig. 17. Kinematic input (ω_r), rotational velocity of the right wheel of the tractor; experimental implementation results.

https://doi.org/10.1017/S0263574716000886 Published online by Cambridge University Press

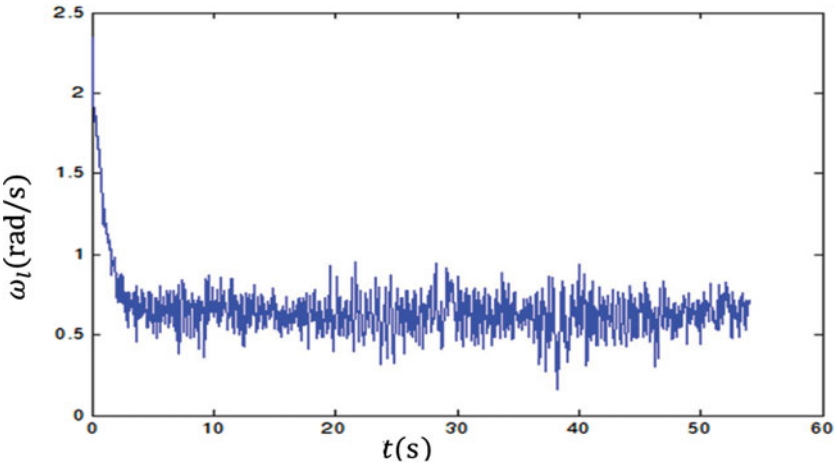

Fig. 18. Kinematic input (ω_l), rotational velocity of the left wheel of the tractor; experimental implementation results.

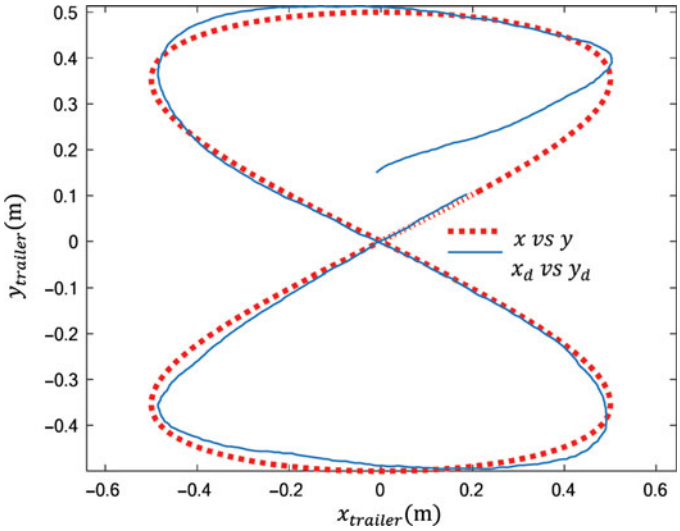

Fig. 19. Tracking desired 8 type trajectories in cartesian space for the trailer; experimental implementation results.

References

1. R. Siegwart, I. R. Nourbakhsh and D. Scaramuzza, *Introduction to Autonomous Mobile Robots* (MIT Press, Massachusetts, 2011).
2. K. Alipour and S. A. A. Moosavian, "Effect of terrain traction, suspension stiffness and grasp posture on the tip-over stability of wheeled robots with multiple arms," *J. Adv. Robot.* **26**(8–9), 817–842 (2012).
3. K. Alipour and S. A. A. Moosavian, "How to ensure stable motion of suspended wheeled mobile robots," *J. Ind. Robot.* **38**(2), 139–152 (2011).
4. K. Alipour, S. A. A. Moosavian and Y. Bahramzadeh, "Dynamics of wheeled mobile robots with flexible suspension: Analytical model and verification," *Int. J. Robot. Autom.* **23**(4), 242–250 (2008).
5. G. Campion, G. Bastin and B. D. Novel, "Structural properties and classification of kinematic and dynamic models of wheeled mobile robots," *IEEE Trans. Robot. Autom.* **12**(1), 47–62 (1996).
6. N. H. McClamroch and I. Kolmanovsky, "Developments in nonholonomic control problems," *IEEE Control Syst*. **15**, 20–36 (1995).
7. L. Lapierre, R. Zapata and P. Lepinay, "Combined path-following and obstacle avoidance control of wheeled robot," *The Int. J. Robot. Res.* **26**(4), 361–375 (2007).
8. S. Sun and P. Cui, "Path tracking and a partical point stabilization of mobile robot," *Robot. Comput.-Integr. Manuf.* **20**(1), 29–34 (2004).
9. C. Prieur and A. Astolfi, "Robust stabilization of chained systems via hybrid control," *IEEE Trans. Autom. Control*, **48**(10), 1768–1772 (2003).
10. C. Wang, "Semiglobal practical stabilization of nonholonomic wheeled mobile robots with saturated inputs," *Automatica*, **44**(3), 816–822 (2008).

https://doi.org/10.1017/S0263574716000886 Published online by Cambridge University Press

11. C. Y. Chen, T. H. S. Li, Y. C. Yeh and C. C. Chang, "Design and implementation of an adaptive sliding-mode dynamic controller for wheeled mobile robots," *Mechatronics*, **19**(2), 156–166 (2009).
12. F. N. Matins, W. C. Celeste, R. Carelli, M. Sarcinelli-Filho and T. F. Bastosfilho, "An adaptive dynamic controller for autonomous mobile robot trajectory tracking," *Control Eng. Pract.* **16**(11), 1354–1363 (2008).
13. E. Yang, D. Gu, T. Mita and H. Hu, "Nonlinear Tracking Control of a Car-Like Mobile Robot Via Dynamic Feedback Linearization," *Proceeding of Control Conference*, Bath, United Kingdom (2004).
14. C.-Y. Chen, T.-H. S. Li, Y.-C. Yeh and C.-C. Chang, "Design and implementation of an adaptive sliding-mode dynamic controller for wheeled mobile robots," *Mechatronics*, **19**(2), 156–166 (2009).
15. J. Huang, C. Wen, W. Wang and Z.-P. Jiang, "Adaptive output feedback tracking of a nonholonomic mobile robot," *Automatica*, **50**(3), 821–831 (2014).
16. D. Chwa, "Fuzzy adaptive tracking control of wheeled robots with stat-dependent kinematic and dynamic disturbances," *IEEE Trans. Fuzzy Syst.* **20**(3), 587–593 (2012).
17. T. McGeer, "Passive dynamic walking," *Int. J. Robot. Res.* **9**(2), 62–82 (1990).
18. K. Y. Wichlund, O. J. Sørdalen and O. Egeland, "Control of Vehicles with Second-Order Nonholonomic Constraints: Underactuated Vehicles," *Proceedings of the European Control Conference*, Rome, Italy (1995) pp. 3086–3091.
19. M. W. Spong, "Modeling and control of elastic joint robots," *Trans. ASME, J. Dyn. Syst. Meas. Control*, **109**, 310–319 (Dec. 1987).
20. M. W. Spong, "Underactuated Mechanical Systems," *Proceedings of the Control Problems in Robotics and Automation* (Springer, Berlin Heidelberg, 1998) pp. 135–150.
21. M. Yue, P. Hu and W. Sun, "Path following of a class of non-holinomic mobile robot with underactuated vehicle bod," *IET Control Theory & Appl*. **4**(10), 1898–1904 (2010).
22. P. Oryschuk, A. Salerno, A. M. Al-Husseini and J. Angeles, "Experimental validation of an underactuated two-wheeled mobile robot," *IEE/ASME Trans. Mechatronics*, **14**(2), 252–257 (2009).
23. A. Khanpoor, A. K. Khalaji and S. A. A. Moosavian, "Dynamics Modeling and Control of a Wheeled Mobile Robot with Omni-Directional Trailer," *22nd Iranian Conference on, Electrical Engineering (ICEE*), Tehran, Iran (2014) pp. 1254–1259.
24. A. K. Khalaji and S. A. A. Moosavian, "Robust adaptive controller for a Tractor-Trailer mobile robot," *IEEE/ASME Trans. Mechatronics*, **19**(3), 943–953 (2014).
25. A. K. Khalaji and S. A. A. Moosavian, "Adaptive sliding mode control of a wheeled mobile robot towing a trailer," *Proc. Inst. Mech. Eng. Part I: J. Syst. Control Eng.* **229**(2), 169–183 (2015).
26. A. K. Khalaji, M. R. Bidgoli and S. A. A. Moosavian, "Non-Model Based Control for a Wheeled Mobile Robot Towing Two Trailers," *Proceeding of the Institution of Mechanical Engineers, Part K: Journal of Multi-body Dynamics*, **229**(1), 97–108 (2014).
27. K. M. Hangos, J. Bokor and G. Szederkenyi, *Analysis and Control of Nonlinear Process Systems* (Springer Science & Business Media, London, 2004).

https://doi.org/10.1017/S0263574716000886 Published online by Cambridge University Press